Paper AAS 99-469

Entry Dispersion Analysis for the Genesis Sample Return Capsule

Prasun N. Desai and F. McNeil Cheatwood

NASA Langley Research Center
Hampton, VA

AAS/AIAA Astrodynamics Specialist Conference

Girdwood, Alaska 16-19 August 1999

AAS Publications Office, P.O. Box 28130, San Diego, CA 92129

AAS 99-469

ENTRY DISPERSION ANALYSIS FOR THE GENESIS SAMPLE RETURN CAPSULE

Prasun N. Desai* and F. McNeil Cheatwood*
p.n.desai@larc.nasa.gov, f.m.cheatwood@larc.nasa.gov

Genesis will be the first mission to return samples from beyond the Earth-Moon system. The spacecraft will be inserted into a halo orbit about the L1 (Sun-Earth) libration point where it will remain for two years collecting solar wind particles. Upon Earth return, the sample return capsule, which is passively controlled, will descend under parachute to Utah. The present study describes the analysis of the entry, descent, and landing scenario of the returning sample capsule. The robustness of the entry sequence is assessed through a Monte Carlo dispersion analysis where the impact of off-nominal conditions is ascertained. The dispersion results indicate that the capsule attitude excursions near peak heating and drogue chute deployment are within Genesis mission limits. Additionally, the size of the resulting 3-σ landing ellipse is 47.8 km in downrange by 15.2 km in crossrange, which is within the Utah Test and Training Range boundaries.

INTRODUCTION

The fifth of NASA's Discovery class missions is a sample return mission known as Genesis. The spacecraft will be inserted into a halo orbit about the L1 (Sun-Earth) libration point where it will remain for two years collecting solar wind particles (Figure 1). Genesis is scheduled to be launched in January of 2001 and will be the first mission to return samples from beyond the Earth-Moon system. Upon Earth return in August 2003, the entry capsule (Figure 2) containing the solar wind samples, will be released from the main spacecraft (decelerating with the aid of a parachute) for a mid-air recovery in Utah over the U.S. Air Force's Utah Test and Training Range (UTTR). Due to the similarities between the Genesis and Stardust[1] missions (i.e., returning a sample capsule to Earth, decelerating with the aid of a parachute, and landing at UTTR), the Genesis entry builds upon

Figure 1 Genesis Spacecraft Sampling Configuration

*Aerospace Engineer, Aerospace Systems Concepts and Analysis Competency, NASA Langley Research Center, Hampton, VA 23681-2199

the Stardust entry, descent, and landing scenario.[2,3] As with the Stardust mission, approximately four hours prior to entry, the sample return capsule (SRC) will be spun-up to 16 rpm and separated from the main spacecraft. The SRC has no active control system, so the spin-up is required to maintain its entry attitude (nominal 0 deg angle-of-attack) during coast. Throughout the atmospheric entry, the passive SRC will rely solely on aerodynamic stability for performing a controlled descent through all aerodynamic flight regimes: hypersonic-rarefied, hypersonic-transitional, hypersonic-continuum, supersonic, transonic, and subsonic. The SRC must possess sufficient aerodynamic stability to overcome the gyroscopic (spin) stiffness in order to minimize any angle-of-attack excursions during the severe heating environment. Additionally, this stability must persist through the transonic and subsonic regimes to maintain a controlled attitude at parachute deployment.

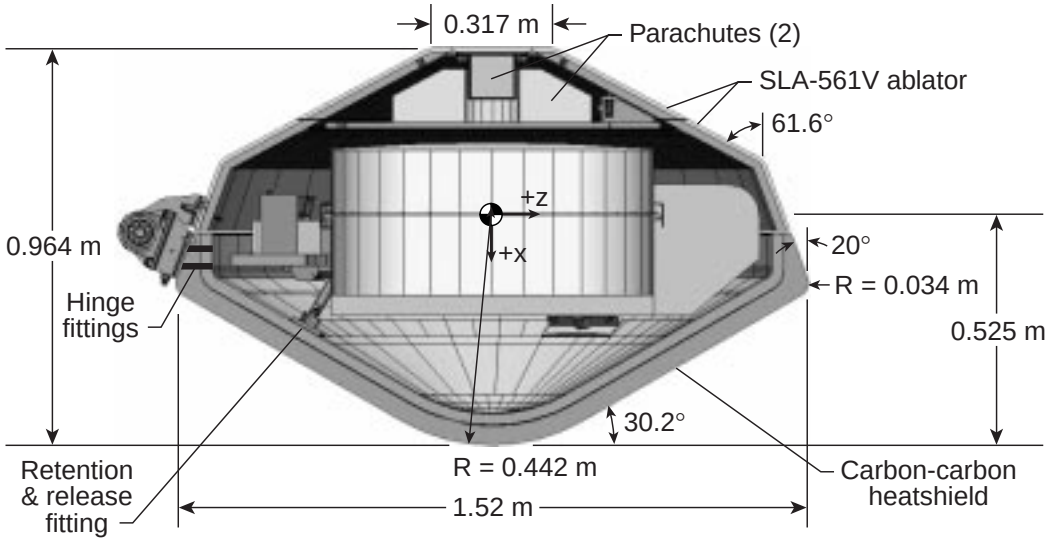

Figure 2 Genesis SRC Configuration

This paper analyzes the entry, descent, and landing sequence for the returning sample capsule. The analysis is performed through a trajectory simulation of the entire entry (from spacecraft separation to landing) to predict the descent attitude and landing conditions. In addition, a Monte Carlo dispersion analysis is performed to ascertain the impact of off-nominal conditions which may arise during the entry in order to determine the robustness of the Genesis SRC design. Specifically, the SRC attitude near peak heating and parachute deployment is of interest, along with the landing footprint ellipse. Note, the landing footprint is of interest rather than the footprint at the air-snatch conditions due to range safety requirements for ensuring that the SRC will land within the boundaries of UTTR in the event of air-snatch failure.

ANALYSIS

Aerodynamics

An aerodynamic database is one of the models required for the flight dynamics simulation. Due to the similarity of the Genesis and Stardust entry capsules (spherically-blunted 60-deg sphere cone forebodies), the Stardust aerodynamic database can serve as the foundation for the Genesis aerodynamic database. That aerodynamic database is constructed from a combination of simple relations such as impact methods and bridging functions, high-fidelity numerical solutions, and ground-based experimental data. The aerodynamic characteristics of the Stardust capsule are described in detail by Mitcheltree, et. al. in Ref. 4, and discussed briefly below.

The entry trajectories of Stardust and Genesis traverse many different flow regimes (hypersonic-rarefied, hypersonic-transitional, hypersonic-continuum, supersonic, transonic, and subsonic). Therefore, the aerodynamic database is constructed from a variety of sources. At the outer reaches of the atmosphere, free molecular flow calculations describe the rarefied aerodynamics. In the transitional flow regime, Direct Simulation Monte Carlo (DSMC) solutions are used to anchor simple bridging functions for the aerodynamic coefficients. In the hypersonic-continuum regime, modified-Newtonian values, anchored with solutions from the computational fluid dynamics (CFD) code LAURA (Langley Aerothermodynamic Upwind Relaxation Algorithm)[5] describe the aerodynamics. At supersonic and transonic speeds, the aerodynamics are based on two sets of existing wind tunnel data. Subsonic aerodynamics are defined by a combination of static wind tunnel measurements and dynamic free flight measurements.[6] These sources are blended to form a cohesive database which describes the aerodynamics of the SRC for the expected flight conditions. Figure 3 shows the range of application of the various aerodynamic sources mentioned above.

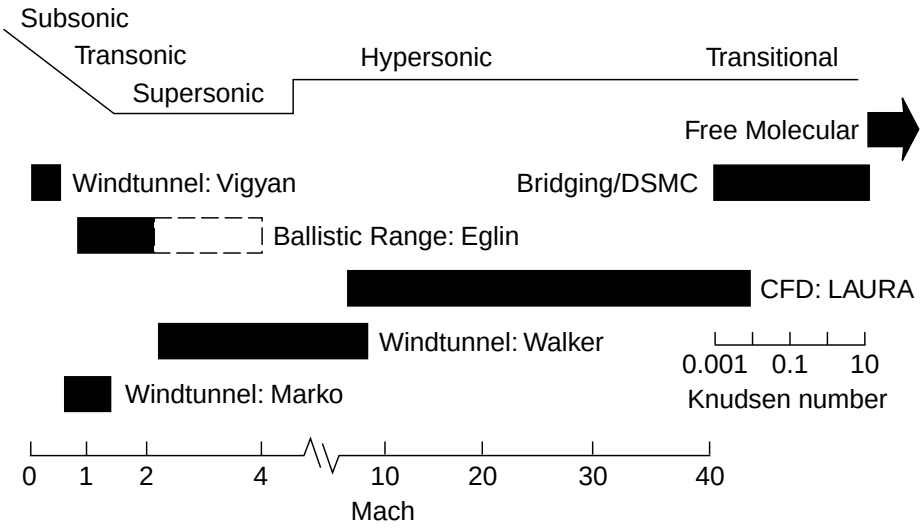

Figure 3 Genesis SRC Aerodynamic Database

While the Stardust and Genesis SRC forebodies are similar, their afterbodies are quite different. Stardust has a 30-deg truncated cone for its afterbody. Genesis, on the other hand, has a bi-conic afterbody whose first cone has a turning angle of 20 deg. As a result, the Stardust aerodynamics database is updated (where appropriate) to reflect these differences.

At hypersonic speeds, the vehicles should have virtually the same aerodynamics characteristics for angles of attack less than 20 deg. Since angles of attack in excess of this level may occur early in the entry trajectory, the free molecular values for Stardust are replaced with results for the Genesis SRC. In the transitional flow regime, several DSMC solutions were performed to confirm that the bridging function tailored to the Stardust entry is appropriate for Genesis as well. For the hypersonic-continuum portion of the entry, the SRC angle of attack will be small, and the Stardust database should again be applicable to Genesis. Examination of CFD solutions verifies that the Stardust database does indeed accurately describe the aerodynamic behavior of the Genesis SRC in this regime. As a result, an update to the aerodynamics in the hypersonic flight regime is not necessary.

As mentioned above, for supersonic, transonic, and subsonic speeds, the Stardust static aerodynamics are based on existing wind tunnel data. These same values are used for Genesis, and the uncertainties placed on the aerodynamics (see Table 2) reflect the fact that the afterbodies are different. The Genesis SRC supersonic and transonic aerodynamics are being further characterized using ballistic range tests which are presently being conducted. When analysis of these test results is completed, the aerodynamic database will be updated (as noted by dashed region in Figure 3).

Trajectory Simulation

The trajectory analysis is performed using the six- and three-DOF (degree-of-freedom) versions of the Program to Optimize Simulated Trajectories (POST).[7] This program has been utilized previously for similar applications.[8-10] The three-DOF program (which integrates the translation equations of motion) is used from spacecraft separation to atmospheric interface. The six-DOF version of POST (which integrates the translational and rotational equations of motion) is used from atmospheric interface to parachute deployment. The three-DOF program is used again from parachute deployment to landing. The trajectory simulation includes Earth atmospheric (GRAM-95)[11] and gravitational models, capsule separation and non-instantaneous parachute deployment models, as well as capsule aerodynamics and mass properties. The validity of the present approach has been demonstrated recently through comparisons between the Mars Pathfinder pre-flight predictions of the flight dynamics and the actual flight data.[12]

During the entry, off-nominal conditions may arise which affect the descent profile. These off-nominal conditions can originate from numerous sources: 1) capsule mass property measurement uncertainties, 2) separation attitude and attitude rate uncertainties, 3) limited knowledge of the flight-day atmospheric properties (density, pressure, and winds), 4) computational uncertainty with the aerodynamic analysis, and 5) uncertainties with para-

chute deployment. In this analysis, an attempt is made to conservatively quantify and model the degree of uncertainty in each mission parameter. For this mission, 47 potential uncertainties were identified. These uncertainties are grouped into two categories: exo-atmospheric and atmospheric. Tables 1 and 2 list these uncertainties, respectively, along with the corresponding 3-σ variances. For most of the parameters, a Gaussian distribution is sampled. However, for the radial center-of-gravity (c.g.) offset quadrant and parachute deployment parameters (gravity-switch, timers, and aerodynamics), uniform distributions are utilized to model their operating performance.

Note, although the dispersions in the mass and major moments of inertia of the capsule will be much smaller as launch approaches, large variances are presently used to account for potential variations in the SRC design. Additionally, the dispersion in the SRC separation from the main spacecraft is split into two sources: 1) uncertainties during the capsule separation process itself, and 2) uncertainties arising from the spacecraft propulsive attitude maneuver that positions the SRC to the proper orientation for release.

Table 1

EXO-ATMOSPHERIC MISSION UNCERTAINTIES

Mass Properties	3-σ Variance
Mass	±1.0 kg
cg position along spin axis	±0.0254 cm (0.01 in.)
cg position off spin axis	±0.0254 cm (0.01 in.)
Major moment of inertia (I_{xx}, I_{yy}, I_{zz})	±10%, 20%, 20%
Cross products of inertia (I_{xy}, I_{xz}, I_{yz})	±0.11 kg-m^2, ±1.1 kg-m^2, ±0.1 kg-m^2

Separation State Vector		
Position, Velocity	correlated with covariance matrix producing a $\Delta\gamma_i$ =	±0.06 deg
Pitch/yaw attitude		±2.69 deg
Pitch/yaw rate		±4.24 deg/s
Roll rate		±1 rpm

Separation		
Spring induced ΔV:	Body x-axis ΔV	±0.0305 m/s (1.2 in/s)
	Body y-axis ΔV	±0.0203 m/s (0.8 in/s)
	Body z-axis ΔV	±0.0203 m/s (0.8 ins)
Precession induced ΔV:	Body x-axis ΔV	±0.049 m/s (1.9 in/s)
	Body y-axis ΔV	±0.014 m/s (0.6 in/s)
	Body z-axis ΔV	±0.014 m/s (0.6 in/s)

Table 2

ATMOSPHERIC MISSION UNCERTAINTIES

Aerodynamic	3-σ Variance
Free molecular aerodynamics, C_A	±10%
C_N, C_Y	±8%
C_m, C_n	±12%
Hypersonic continuum aerodynamics, C_A	±4%
C_N, C_Y	±8%
C_m, C_n	±10%
Supersonic continuum aerodynamics, C_A	±10%
C_N, C_Y	±5%
C_m, C_n	±8%
Subsonic continuum aerodynamics, C_A	±5%
*Hypersonic dynamic stability coefficients, C_{mq}, C_{nq}	±0.28
*Supersonic dynamic stability coefficients, C_{mq}, C_{nq}	±0.2
Atmosphere	
Pressure, density, winds: GRAM-95 model	3-σ scale factor
Other	
*Drogue chute g-switch	±10%
*Drogue chute deployment timer	±0.05 sec
*Drogue chute aerodynamics, C_A	±10%
*Main chute deployment timer	±0.05 sec
*Main chute aerodynamics, C_A	±10%

*Uncertainty sampled using uniform distribution

RESULTS AND DISCUSSION

Nominal Mission

As was the case for the Stardust capsule, the Genesis SRC is aerodynamically unstable in the hypersonic-rarefied and supersonic flight regimes due to the capsule's rearward center-of-gravity location. This aft center-of-gravity location produces a static instability in the free molecular regime, while near transonic speeds, a dynamic instability exists. References 4, 6 and 13 discuss these aerodynamic instabilities in greater detail. If these instabilities are not addressed, large angle of attack excursions could result during the entry. To mitigate the effects of these instabilities, the Genesis entry sequence relies on the Stardust entry, descent, and landing scenario that was developed to successfully traverse all flight regimes. Figure 4 shows the entry sequence, with the terminal descent phase highlighted. References 2 and 3 give an in-depth description on the development of the entry scenario utilizing the high entry spin rate, as well as the use of a supersonic drogue parachute deployment.

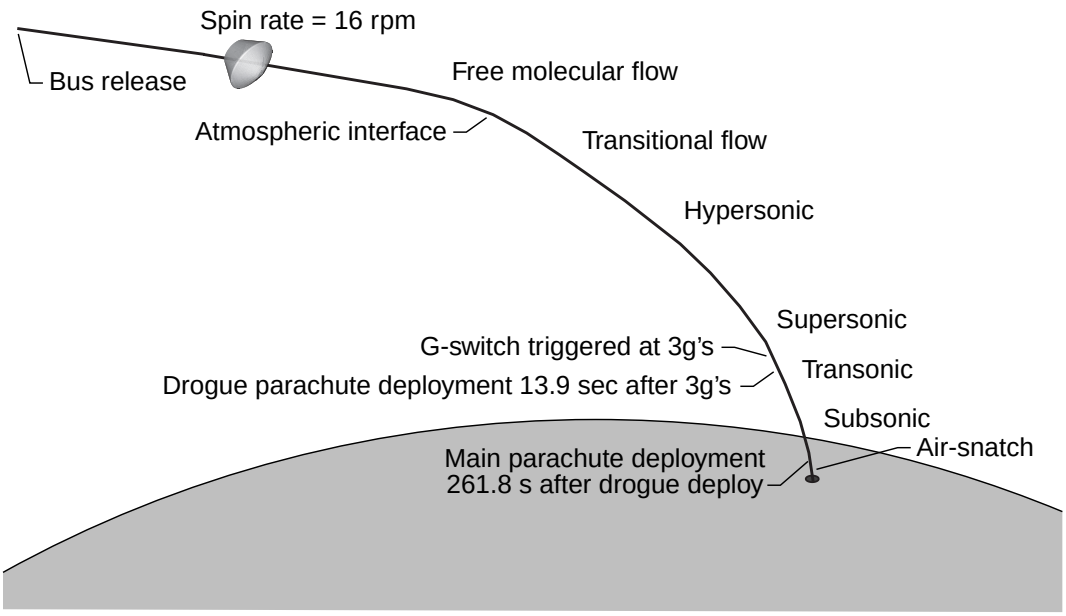

Figure 4 Nominal Genesis SRC Entry Sequence

Upon Earth entry, the entry profile utilizes a g-switch (i.e. gravity-switch) and two timers for deployment of the drogue and main parachutes. The g-switch is triggered after sensing 3 g's. At that point, the drogue timer is initiated. After 13.9 seconds, the drogue chute is deployed (approximately Mach 1.4), and the main timer is initiated. After 261.8 seconds (approximately at 6 km), the main parachute is deployed. The entry scenario calls for an air-snatch of the SRC at an altitude of approximately 2.5 km. The above event times are based on the nominal SRC mass properties given in Table 3. This nominal entry sequence is sufficiently robust to accommodate off-nominal conditions during the descent (as confirmed by the Monte Carlo analysis presented in a later section).

Table 3

NOMINAL MASS PROPERTIES FOR THE SRC

Mass, kg	225
Center of gravity, m	
Along spin axis (x-direction, from nose)	0.525 (x_{cg}/D = 0.345)
Off spin axis (y-direction)	0.0011
Off spin axis (z-direction)	0.0022
I_{xx}, kg-m^2 (spin axis)	46.7
I_{yy}, kg-m^2	31.7
I_{zz}, kg-m^2	33.5
I_{xy}, kg-m^2	0.0
I_{xz}, kg-m^2	0.0
I_{yz}, kg-m^2	0.0

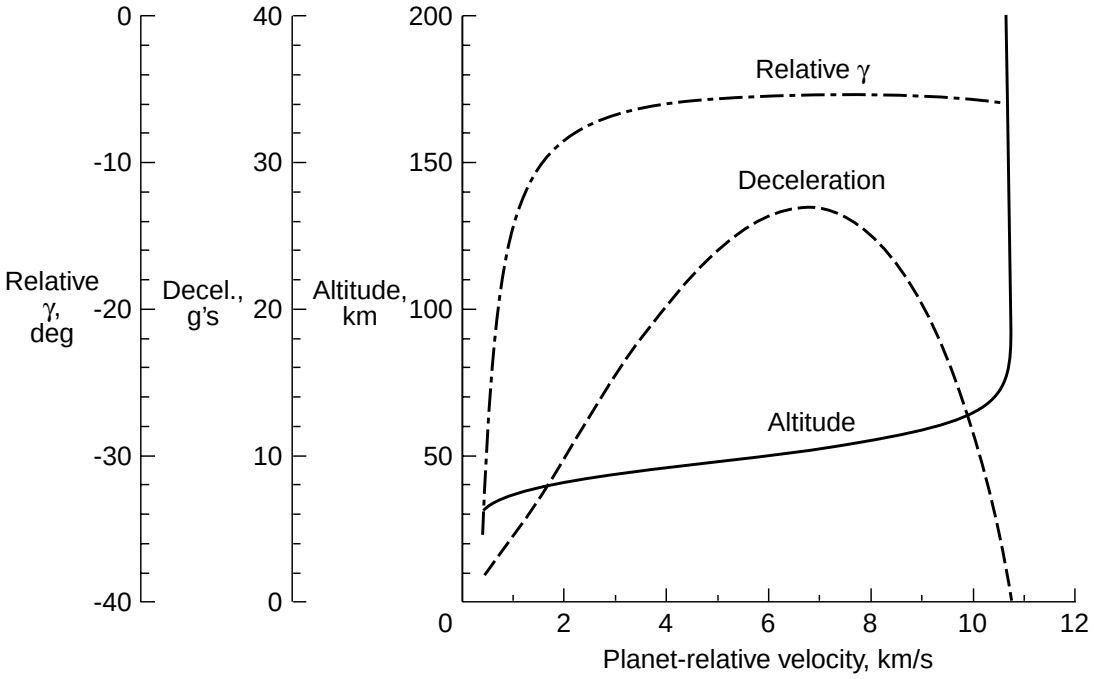

Figure 5 Nominal Entry Sequence

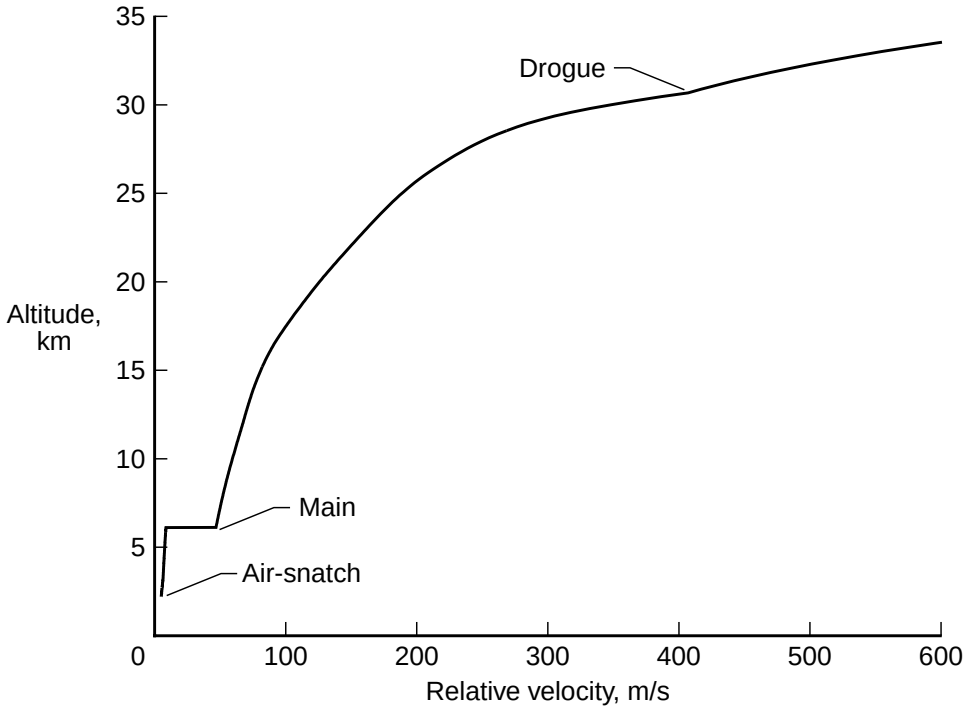

Figure 6 Nominal Entry Parachute Deployment Sequence

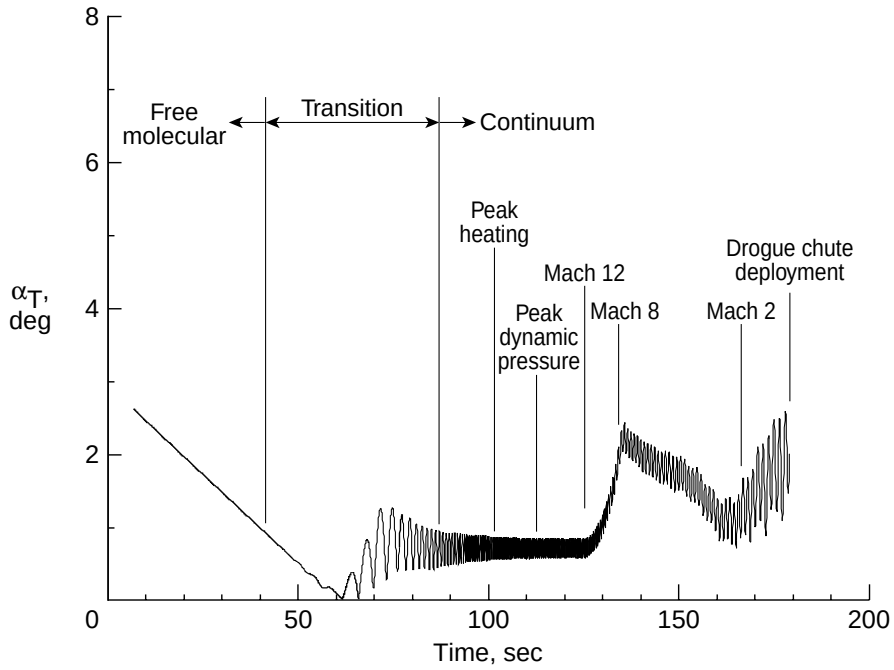

Figure 7 Nominal SRC Attitude Profile

The flight characteristics of the nominal entry are shown in Figures 5-7. The planet-relative entry flight-path angle (γ_r) and velocity (referenced to a radius of 6503.14 km) are –8.25 deg and 10.7 km/s, respectively. The maximum deceleration experienced by the SRC during the descent is 26.9 g's. Beginning at Mach 1.4 (approximately 30 km altitude), the terminal descent phase of the entry begins. Figure 6 shows the nominal altitudes of the drogue and main parachute deployments.

Similar to the Stardust entry, the Genesis SRC is spun-up to 16 rpm and released from the main spacecraft. Unlike Stardust, the high spin rate of the Genesis SRC, coupled with its larger moments of inertia, provide sufficient gyroscopic stiffness to allow the capsule to traverse the hypersonic-rarefied flight regime without experiencing large angles of attack in the transitional flow regime. As seen in Figure 7, the attitude of the capsule in the transitional flow regime does not exceed 1 deg (compared to 7 deg for Stardust). The total angle-of-attack (α_T), which is the included angle between the capsule spin-axis and the atmospheric-relative velocity vector, is observed to be approximately 0.8 deg near peak heating (which occurs around Mach 30). As the SRC descends, the static margin decreases near Mach 12 producing a new trim angle of attack, because the capsule has a non-zero radial c.g. off-set from the spin axis. Consequently, an increase in α_T, from approximately 0.8 deg near Mach 12 to approximately 1.2 deg near Mach 2, is observed. In transitioning to a new trim point, attitude rates induce an overshoot in α_T (peaking around Mach 8) before receding around Mach 2. As the SRC approaches transonic speeds, the dynamic instability (which is inherent to blunt bodies such as the present capsule configuration) produces an increase in α_T until drogue chute deployment (Refs. 2, 3 and 6 describe the impact of this dynamic instability in greater detail).

Monte Carlo Dispersion Analysis

Independent Uncertainty Effects. Before a combination of off-nominal conditions are examined, a sensitivity analysis is first performed to identify the mission uncertainties which have the greatest impact on the overall landing footprint. Each of the 47 mission uncertainties are independently set at their respective ±3-σ (maximum/minimum) variances. Figure 8 shows the resulting total downrange obtained from the largest contributors to the overall landing footprint. The top four contributors, containing uncertainties in initial state vector and atmospheric wind and density, contribute on the order of 15-20 km each to the landing footprint size. The remaining uncertainties (containing dispersions in spacecraft separation velocity, capsule and parachute aerodynamic drag) produce downrange dispersions of approximately 1-5 km each. Those mission uncertainties that are not depicted lead to downrange dispersions less than 0.5 km.

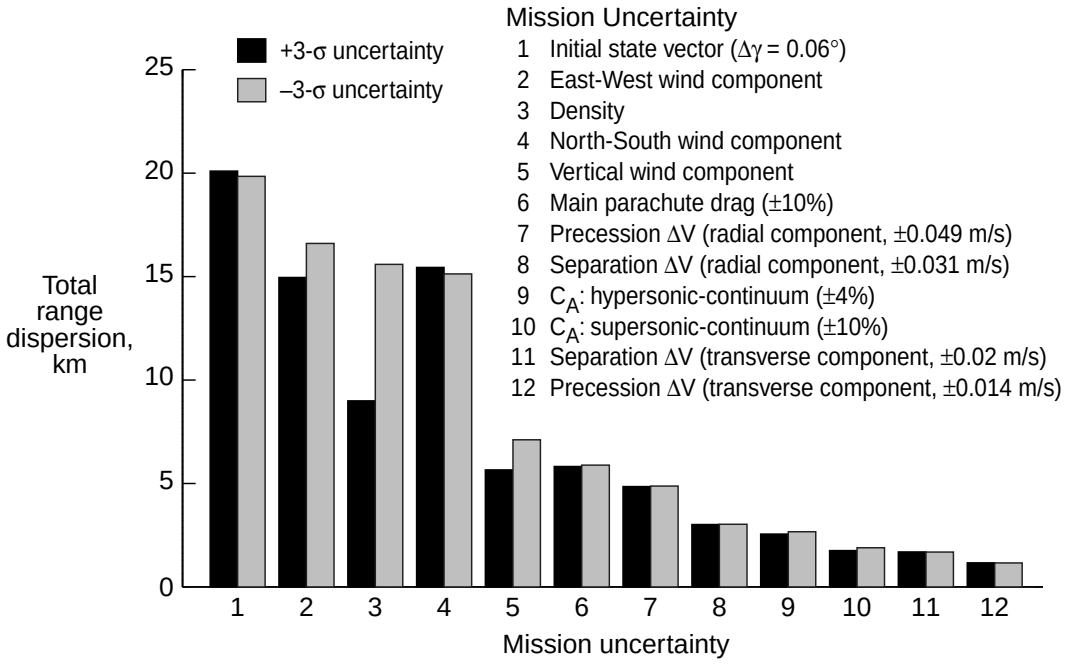

Figure 8 Major Contributors to Total Range Dispersion (3-σ variance shown in parenthesis)

Multiple Uncertainty Effects. To determine the robustness of the Genesis SRC entry profile, off-nominal conditions are simulated to address uncertainties which may arise during the descent. The impact of multiple uncertainties occurring simultaneously is ascertained by performing a Monte Carlo dispersion analysis. Three thousand random, off-nominal trajectories are simulated to assure proper Gaussian or uniform distributions for the 47 mission uncertainties identified.

The statistical results from the 3000 Monte Carlo simulations are displayed in Figures 9-16. Figures 9-11 show the distribution of the total angle-of-attack at three discrete locations during the early phase of the mission: at atmospheric interface, in the transitional re-

gime, and at peak heating. At atmospheric interface, the statistical mean total angle-of-attack of the 3000 Monte Carlo cases is 2.7 deg. The maximum α_T observed is around 6.8 deg (which is below the mission constraint of 10 deg). In the transitional regime, the total angle-of-attack does increase (due to the free molecular instability) from atmospheric interface. However, the mean α_T observed is only 4.2 deg, while the maximum α_T is 8.9 deg. These values are much lower than the values of 8.5 deg and 28 deg, respectively, calculated for the Stardust capsule. The higher moments of inertia of the Genesis capsule provide greater gyroscopic stiffness which retard the effects of the instability. As the SRC descends towards peak heating (where it is stable), the mean α_T decreases to 1.5 deg as seen in Figure 11. The maximum α_T observed at peak heating is 3.1 deg (which is below the mission constraint of 10 deg).

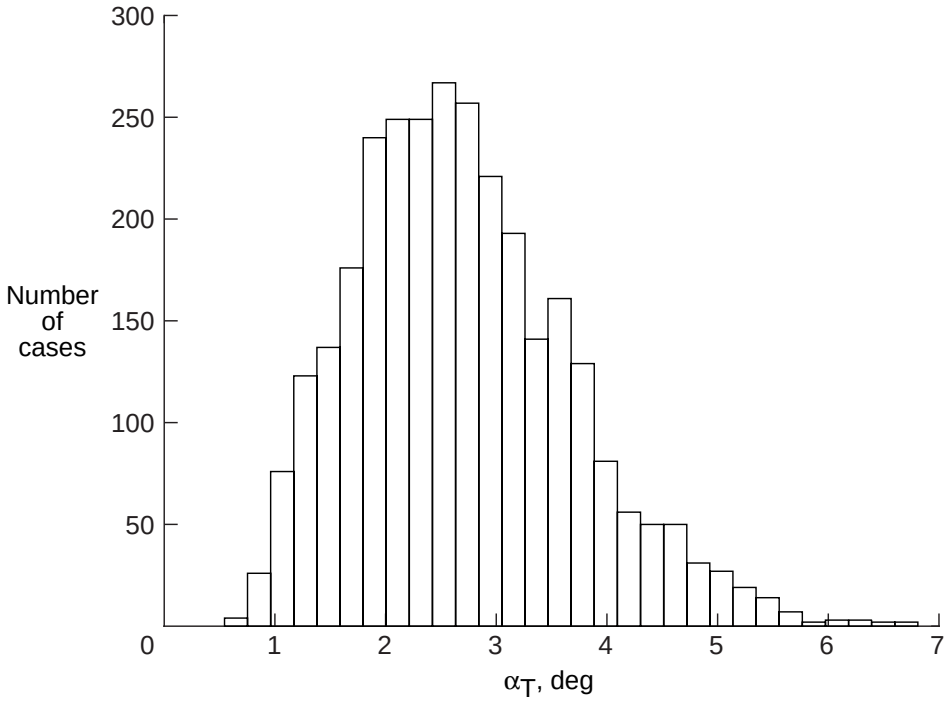

Figure 9 Distribution of Total Angle-of-Attack at Atmospheric Interface Resulting from 3000 Monte Carlo Simulation Cases

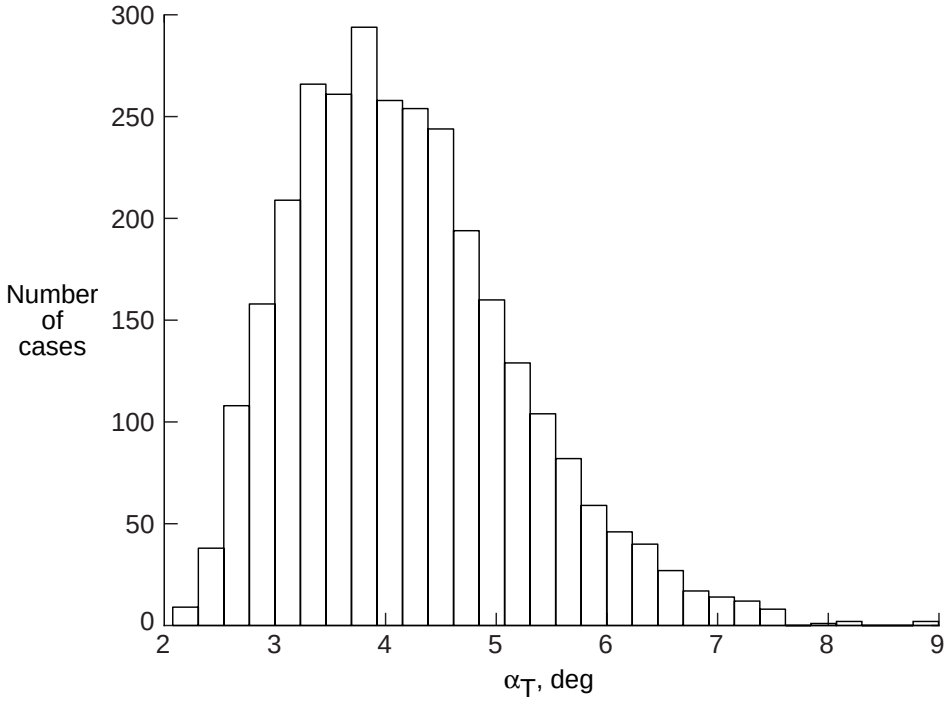

Figure 10 Distribution of Total Angle-of-Attack in Transitional Regime Resulting from 3000 Monte Carlo Simulation Cases

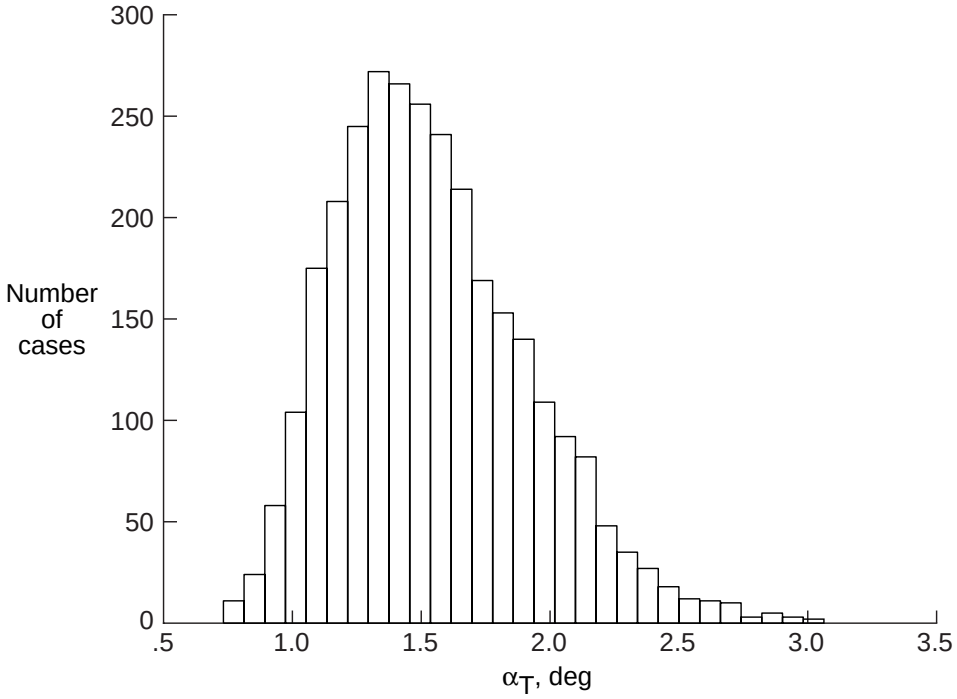

Figure 11 Distribution of Total Angle-of-Attack at Peak Heating Resulting from 3000 Monte Carlo Simulation Cases

Figures 12-14 show the distribution of the drogue and main parachute deployment conditions. The mean Mach number at drogue chute deployment is 1.36, as seen in Figure 12. The minimum deployment Mach number encountered is 1.21, which is high enough to avoid the significant effects of the transonic dynamic instability. The corresponding mean total angle-of-attack at drogue chute deployment (see Figure 13) is 4.1 deg. The maximum α_T observed is 24.6 deg, which is below the mission constraint of 30 deg. Figure 14 shows the distribution of the main parachute deployment altitude. The mean deployment altitude is 6.1 km, with a minimum occurring at 5.4 km.

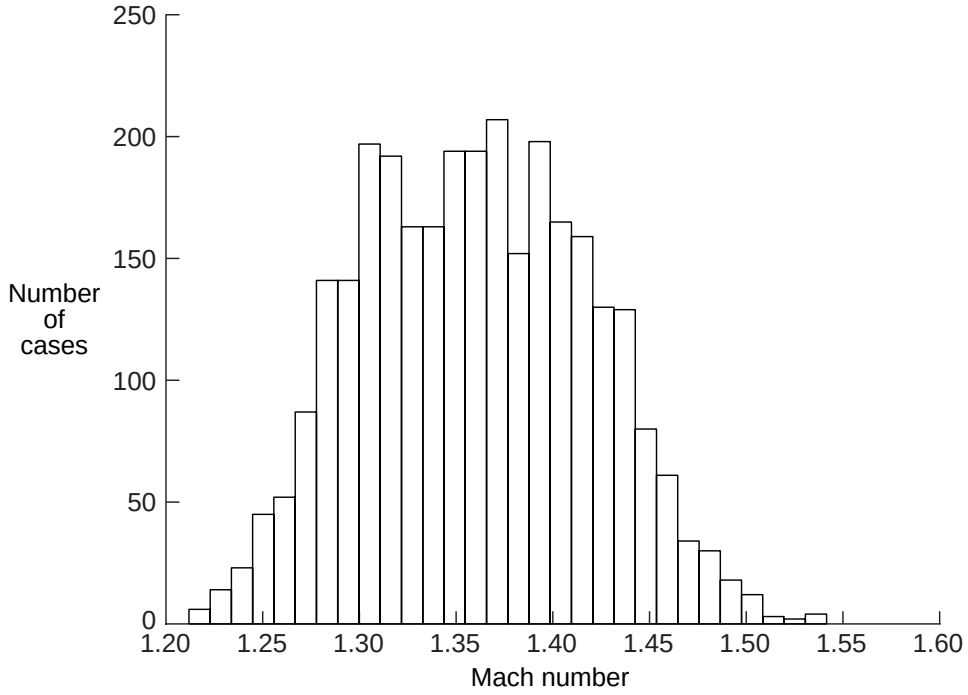

Figure 12 Distribution of Mach Number at Drogue Chute Deployment Resulting from 3000 Monte Carlo Simulation Cases

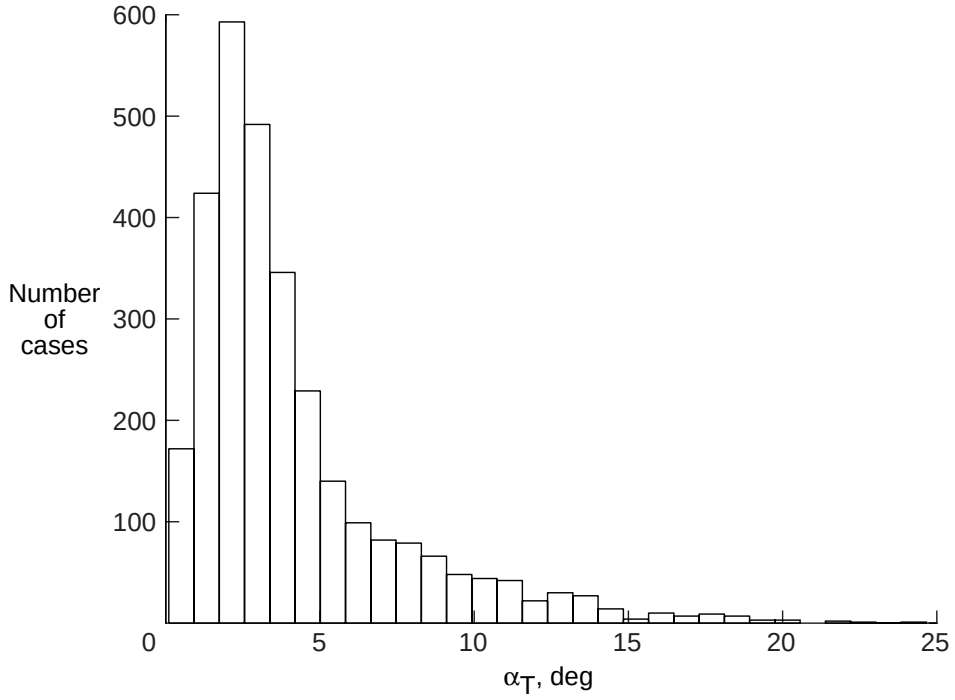

Figure 13 Distribution of Total Angle-of-Attack at Drogue Chute Deployment Resulting from 3000 Monte Carlo Simulation Cases

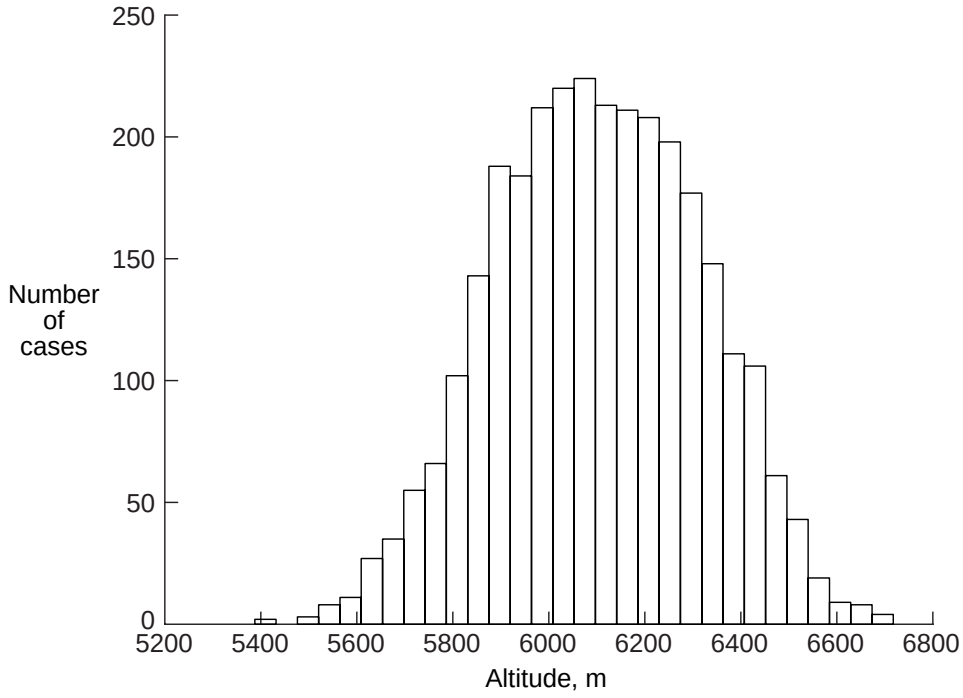

Figure 14 Distribution of Altitude at Main Chute Deployment Resulting from 3000 Monte Carlo Simulation Cases

The downrange and crossrange distributions at landing for the 3000 Monte Carlo cases are illustrated in Figures 15 and 16, respectively. The minimum downrange is –26.3 km (short) from the nominal landing point, whereas the maximum downrange is 30.4 km (long). The maximum crossrange obtained is 8.2 km from the nominal landing point. The resulting 3-σ ellipse has a major axis of 47.9 km (–23.4 short, 24.5 long) in downrange and a minor axis of 15.2 km in crossrange. This footprint is within the UTTR site. Within the assumptions of the present analysis, a 99.7 percent probability exists that the SRC will land within this footprint ellipse. Figure 17 shows the landing location of all 3000 Monte Carlo cases. Table 4 summaries these results. As the capsule design matures and the aerodynamics characteristics of the SRC are updated, the landing footprint will be refined.

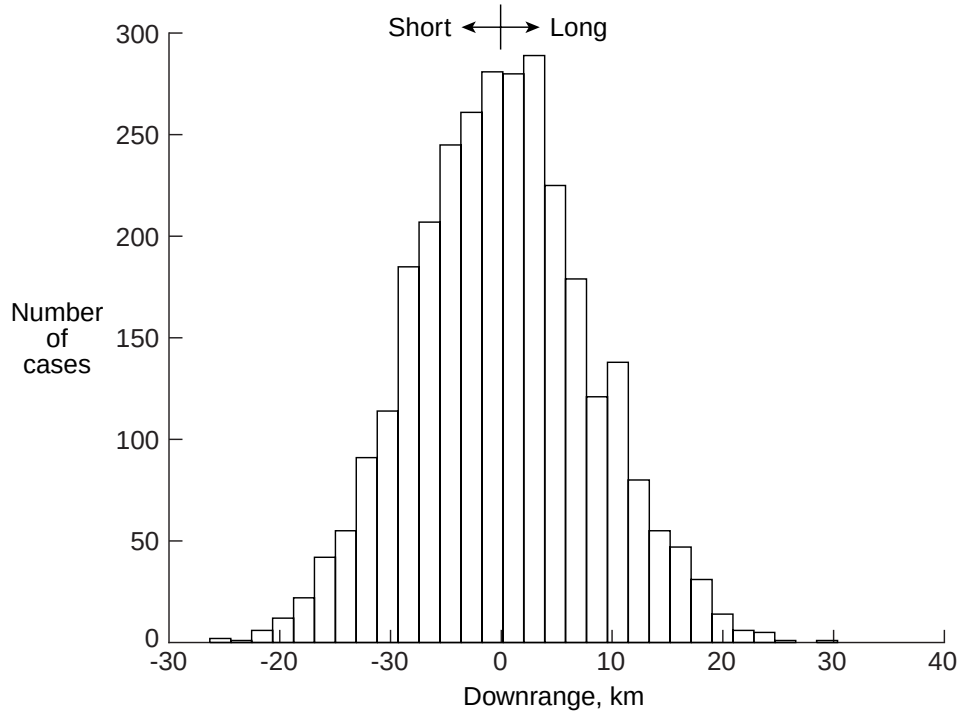

Figure 15 Downrange Distribution at Landing Resulting from 3000 Monte Carlo Simulation Cases

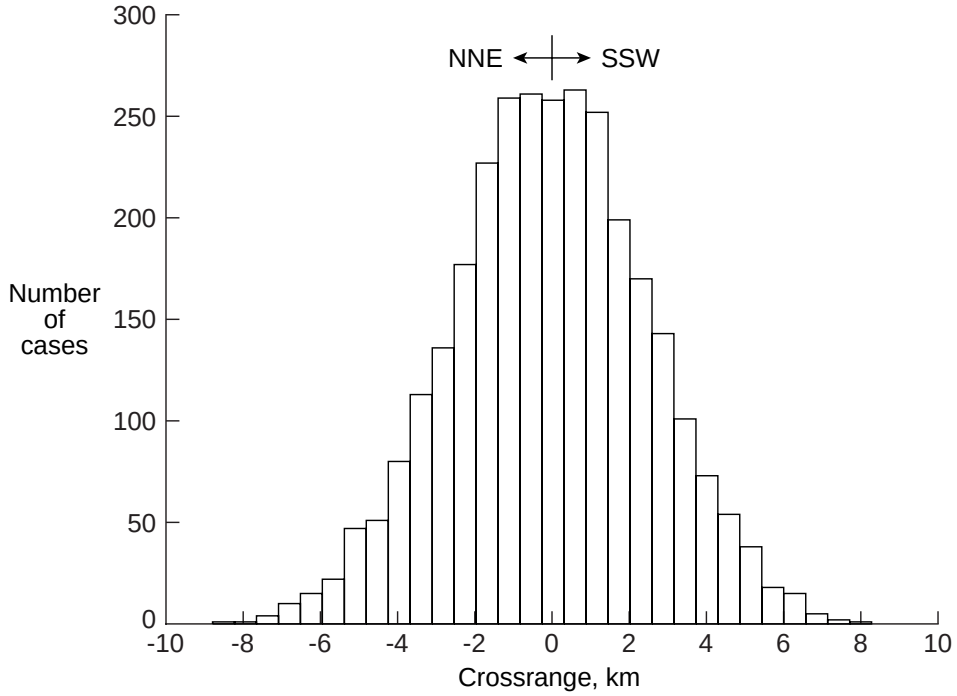

Figure 16 Crossrange Distribution at Landing Resulting from 3000 Monte Carlo Simulation Cases

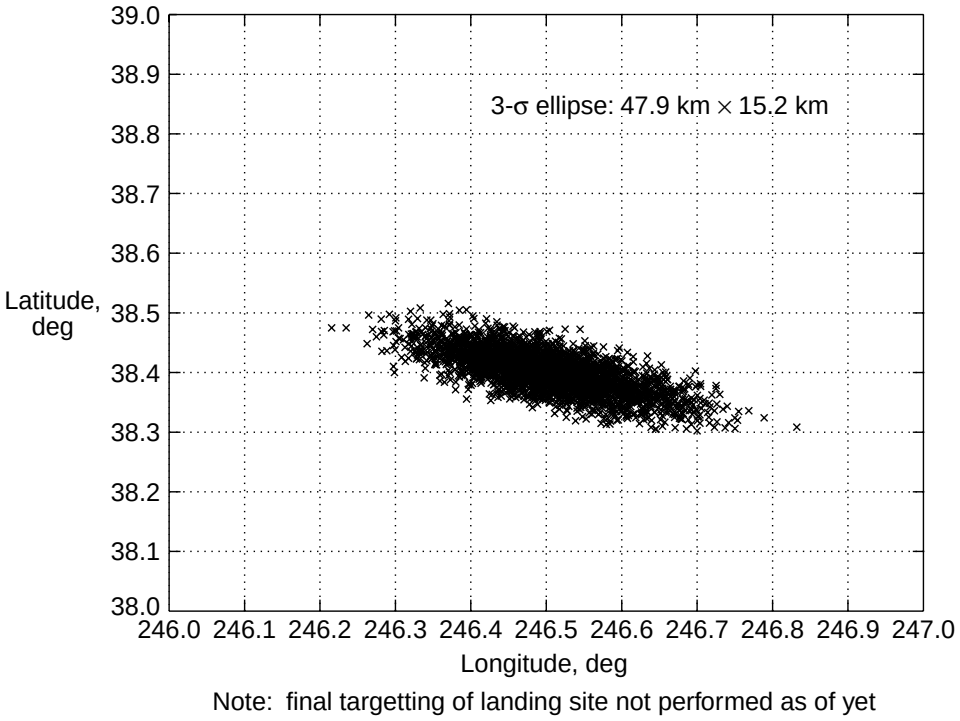

Figure 17 Landing Range Dispersion Resulting from 3000 Monte Carlo Simulation Cases

Table 4

SUMMARY OF MONTE-CARLO ANALYSIS

	Mean	Min.	Max.	3-σ	
Attitude dispersion					
Atmospheric interface α_T, deg	2.7	0.5	6.8	2.9	
Transitional regime α_T, deg	4.2	2.1	8.9	3.1	
Peak heating α_T, deg	1.5	0.7	3.1	1.2	
Drogue chute deployment α_T, deg	4.1	0.1	24.6	10.1	
Landing dispersion					
Downrange, km	0.1	-26.3	30.4	24.5	(long)
				-23.4	(short)
Crossrange, km	-0.1	-8.8	8.3	15.2	
Total range, km	7.0	0.2	30.4	13.6	

CONCLUSIONS

Due to the similarities between the Earth entries of Genesis and Stardust, the Genesis sample return capsule utilizes the entry, descent, and landing sequence developed for Stardust. The nominal entry profile utilizes a gravity-switch and two timers for deployment of the drogue and main parachutes. Additionally, due to the similarities of the Genesis and Stardust entry capsules (spherically-blunted 60-deg sphere cone forebodies), the Stardust aerodynamic database can serve as the foundation for the Genesis aerodynamics.

For the Genesis entry, 47 potential uncertainties were identified which could affect the entry. From a sensitivity analysis, uncertainties in the initial state vector and atmospheric properties (density, and North-South and East-West wind components) were found to produce the greatest downrange dispersions on the order of 15-20 km each. A Monte Carlo analysis of 3000 off-nominal trajectories shows that the SRC attitude near peak heating and drogue chute deployment to be within Genesis mission limits. The resulting 3-σ landing footprint obtained was 47.8 km in downrange by 15.2 km in crossrange (which is within the Utah Test and Training Range boundaries). Within the assumptions of the present study, a 99.7 percent probability exists that the Genesis capsule will land within this ellipse. As the capsule design matures, the landing footprint will be refined.

REFERENCES

1. W. H. Willcockson, “Stardust Sample Return Capsule Design Experience,” *Journal of Spacecraft and Rockets*, Vol. 36, No. 3, 1999, pp. 463-469.

2. P. N. Desai, R. A. Mitcheltree, and F. M. Cheatwood, "Entry Dispersion Analysis for the Stardust Comet Sample Return Capsule," *Journal of Spacecraft and Rockets*, Vol. 36, No. 3, 1999, pp. 463-469.

3. P. N. Desai, R. A. Mitcheltree, and F. M. Cheatwood, "Entry Trajectory Issues for the Stardust Sample Return Capsule," International Symposium on Atmospheric Reentry Vehicles and Systems, March 1999, Arcachon, France.

4. R. A. Mitcheltree, R. G. Wilmoth, F. M. Cheatwood, G. J. Brauckmann, and F. A. Greene, "Aerodynamics of Stardust Sample Return Capsule," AIAA Paper 97-2304, June, 1997.

5. F. M. Cheatwood, and P. A. Gnoffo, "User's Manual for the Langley Aerothermodynamic Upwind Relaxation Algorithm (LAURA)," NASA TM 4674, April 1996.

6. R. A. Mitcheltree, and C. M. Fremaux, "Subsonic Dynamics of Stardust Sample Return Capsule," NASA TM 110329, March 1997.

7. G. L. Brauer, D. E. Cornick, and R. Stevenson, "Capabilities and Applications of the Program to Optimize Simulated Trajectories (POST)," NASA CR-2770, Feb. 1977.

8. R. D. Braun, R. A. Mitcheltree, and F. M. Cheatwood, "Mars Microprobe Entry-to-Impact Analysis," *Journal of Spacecraft and Rockets*, Vol. 36, No. 3, 1999, pp. 412-420.

9. A. Mitcheltree, "Mars Pathfinder Mission Six-Degree-of-Freedom Entry Analysis," *Journal of Spacecraft and Rockets*, Vol. 32, No. 6, 1995, pp. 993-1000.

10. P. N. Desai, R. D. Braun, R. W. Powell, W. C. Engelund, and P. V. Tartabini, "Six-Degree-of-Freedom Entry Dispersion Analysis for the METEOR Recovery Module," *Journal of Spacecraft and Rockets*, Vol. 34, No. 3, 1997, pp. 334-340.

11. C. G. Justus, W. R. Jeffries III, S. P. Yung, and D. L. Johnson, "The NASA/MSFC Global Reference Atmospheric Model - 1995 Version (GRAM-95)," NASA TM-4715, Aug. 1995.

12. D. A. Spencer, S. W. Thurman, C. Peng, and P. H. Kallemeyn, "Mars Pathfinder Entry, Descent, and Landing Reconstruction," AAS Paper 98-146, AAS/AIAA Space Flight Mechanics Meeting, Monterey, CA , Feb. 1998.

13. R. A. Mitcheltree, C. M. Fremaux, and L. A. Yates, "Subsonic Static and Dynamic Aerodynamics of Blunt Entry Vehicles," AIAA 99-1020, 37th Aerospace Sciences Meeting and Exhibit, Reno, NV, Jan. 1999.